JOURNAL OF Materials CHEMISTRY

Experimental and computational study of the gas-sensor behaviour and surface chemistry of the solid-solution $Cr_{2-x}Ti_xO_3$ ($x \leqslant 0.5$)

Dirk Niemeyer,[a] David E. Williams,[a] Peter Smith,[b] Keith F. E. Pratt,[b] Ben Slater,[c] C. Richard A. Catlow[c] and A. Marshall Stoneham[d]

[a]*Department of Chemistry, University College London, 20 Gordon St., London UK WC1H 0AJ*
[b]*Capteur Sensors Ltd, Walton Rd, Portsmouth, Hampshire, UK PO6 1SZ*
[c]*The Royal Institution of Great Britain, Davy Faraday Research Laboratory, 21 Albemarle St., London, UK W1S 4BS*
[d]*Department of Physics and Astronomy, University College London, Gower Place, London, UK WC1E 6BT*

Received 23rd July 2001, Accepted 22nd November 2001
First published as an Advance Article on the web 6th February 2002

The solid solution $Cr_{2-x}Ti_xO_3$ is an excellent gas sensor material, with stability of performance over the short and long-term and minor influences of variations of humidity. It is the first new material to be successfully commercialised in large-volume manufacture for sensing of hydrocarbons, volatile organic compounds (VOC), hydrogen and carbon monoxide at low (ppm) concentrations in air since the introduction of SnO_2 for this purpose in the 1960s. The phase limit is at $x \simeq 0.3$–0.4, above which a 2-phase mixture with $CrTiO_3$ is found. Substitution of Ti strongly decreases the electrical conductivity of the porous bodies studied. Surface high-valency Cr, assumed to be Cr^{VI}, whose proportion is decreased by Ti substitution, is detected by XPS. This effect, and the surface segregation of Ti, control the gas sensor behaviour. Defect models of the (0001) and $(10\bar{1}2)$ surfaces have been assessed by computational modelling: in the absence of Ti, one stable defect is a Cr^{VI}–V_{Cr}'''† pair, which is surface segregated at (0001) and contributes to the relatively high p-type conductivity shown by finely porous bodies of Cr_2O_3 at elevated temperature; with Ti addition, a stable defect, also surface segregated, is the complex $(Ti^{\bullet}_{Cr})_3V_{Cr}'''$. Distortion of the arrangement of surface oxygen above the Cr vacancy creates a possible binding site; the high-valency surface cation creates another. It is suggested that the two sites act in concert to promote the dissociation of oxygen and the surface reaction needed for gas sensing.

Introduction

Semiconducting oxides in the form of finely-divided porous bodies or thin films, at elevated temperatures (typically 200–600 °C), show large variations of electrical conductivity in response to the presence of traces of reactive gases in air. Since the commercial introduction in the 1960s of SnO_2-based sensors, and their wide adoption for hazardous gas monitoring (particularly for domestic carbon monoxide alarms), the phenomenon has been extensively studied, with most attention focussed on SnO_2. The disadvantages of SnO_2 are that there is a very strong effect of variations in ambient humidity, and a related drift over both the short and long-term in the baseline and sensitivity. Reproducibility of manufacture has also proved to be a problem.

Whilst most reports in the literature have been directed at understanding and improving the behaviour of SnO_2, there have also been efforts directed at resolving the difficulties through the introduction of new sensor materials. The phenomenon is general to semiconducting oxides and potentially very many materials could be used with advantage. The solid solution material $Cr_{2-x}Ti_xO_3$ (CTO) has proved particularly effective and has recently been successfully commercialised in large-volume manufacture.[1] It differs from SnO_2 in being a p-type conductor: the conductivity decreases in the presence of reducing gases such as carbon monoxide. Its pattern of sensitivity to different gases differs in general from SnO_2 and in particular it does not respond to methane though it does respond well to the higher hydrocarbons. It offers repeatability in manufacture, excellent stability over the short and long-term and small influence of variations in humidity. The purpose of this paper is to present the behaviour of this material particularly in respect of its response to carbon monoxide and to water vapour, to describe critical factors controlling the response and to discuss the surface chemistry which mediates the electrical response.

Phase diagram and defect model

Early phase diagram work on the Cr_2O_3–TiO_2 system reported a series of phases of the form $Cr_2Ti_{n-2}O_{2n-1}$,[2,3] and a phase (the 'E' phase) of nominal composition $Cr_2Ti_2O_7$ with a wide composition range.[3] Above 1300 °C, a two-phase mixture of 'E' and corundum phases is reported to exist over the range 45 to 98 mol% TiO_2 in $CrO_{1.5}$.[4] However Henshaw *et al.*[5] reported a solid solution phase in $Cr_{2-x}Ti_xO_3$ with $x \leqslant 0.4$. Jayaraman *et al.*[6] showed that, over the range $x = 0.1$ to 0.4, the solid solution was the major phase, merging with $CrTiO_3$ as the minor phase. All of these reports used solid state reaction of mixed Cr_2O_3–TiO_2 as the preparation method. Oyama *et al.*[7] prepared CTO by laser-induced explosive chain reaction of CrO_2Cl_2–$TiCl_4$–H_2 in the vapour phase. A complete solid solution in the range up to $x = 0.25$ was found, with lattice parameters showing a small variation (8%) obeying Vegard's law. A defect model for CTO was proposed by Holt and

†The notation (Kroger–Vink notation) means that the vacancy, V_{Cr}, has a triple negative charge with respect to the neutral lattice. Titanium substituted onto a Cr lattice site carries a single positive charge with respect to the neutral lattice, and is written $Ti^{\bullet}_{Cr}$.

Kofstad[8] and by Henshaw *et al.*:[5] Ti substituted on Cr sites with charge compensated by Cr vacancies.

At elevated temperature (>1000 °C), pure Cr_2O_3 behaves as an intrinsic semiconductor, with conductance independent of oxygen partial pressure and with activation energy for conductance 1.86 eV, interpreted as corresponding to a band gap of 3.3 eV and a migration activation energy (see below) of 0.2 eV[9] At lower temperature, more complex behaviour has been reported.[10] Holt and Kofstad[9,10] showed a very small dependence of the conductivity of pure Cr_2O_3 on oxygen partial pressure ($\sigma \sim P_{O_2}^{1/20}$), consistent with earlier literature, and an activation energy for dense specimens of 0.2 eV. They attributed this energy to activation of mobility of the charge carriers. They postulated control of the conductivity at low temperature by extrinsic defects associated with impurities present above the solubility limit, which predicts, for the divalent impurities taken as the example, variation of $\sigma \sim P_{O_2}^{1/8}$. They presumed that the equilibration was very slow, being determined by the very slow migration of lattice defects. For $Cr_{1.98}Ti_{0.02}O_3$, at 1000 °C, they reported p-type conductivity for $P_{O_2} > 10^{-4}$ atm, varying as $P_{O_2}^{1/4}$, and n-type conductivity at lower P_{O_2}, varying as $P_{O_2}^{-1/4}$. At lower temperatures, for highly porous specimens, Henshaw *et al.*[5] showed an increase of activation energy of conductivity with decreasing oxygen partial pressure, and a consequent decrease in magnitude of the power law exponent of the oxygen dependence of conductivity, from $\sigma \sim P_{O_2}^{0.36}$ at 250 °C to $\sigma \sim P_{O_2}^{0.10}$ at 450 °C (close to the value of the exponent observed by Holt and Kofstad[9,10]). They introduced consideration of the surface processes for interpretation of the behaviour of porous bodies at lower temperature, in particular noting the presence of Cr^{VI} species at the surface, detected by XPS. The effect of the surface processes can explain the higher activation energy for conduction shown by porous bodies in comparison with compact specimens. A simple surface trap-limited model for the conductivity, in which oxygen adsorbed from the gas phase onto the crystallites of the finely porous structure acts as an acceptor state and is the major determinant of the electrical conductivity for such specimens, and with O^-_{ads} as the surface state, predicts $\sigma \sim P_{O_2}^{1/2}$ as the limiting case at low temperature. At higher temperature, the conductivity should be determined by the charge carrier equilibria in the bulk of the crystallites, as considered by Holt and Kofstad.[8–10] Both groups showed that Ti substitution caused a significant decrease in the electrical conductivity, also confirmed by Jayaraman *et al.*[6]

Gas sensor properties

The current consensus[11,12] is that the conductivity of porous bodies of semiconducting oxides in air is determined by the trapping of electrons in surface states associated with adsorbed oxygen. If oxygen vacancies or interstitials are immobile in the lattice, then the behaviour is described entirely in terms of the distribution of the electrons between surface and bulk states. The conductivity is sensitive to the presence of trace reactive gases because catalytic surface processes result in a kinetically determined change in the surface coverage of the oxygen surface trap states. If oxygen defects are sufficiently mobile in the lattice, then the conductivity is simply determined by the equilibrium between bulk lattice defects and oxygen in the gas phase, and the sensitivity to trace reactive gases is lost. In intermediate cases, a conductivity sensitive to the presence of trace reactive gases but varying in time as the lattice defects equilibrate is observed. Time-variation of conductivity can also be caused by migration of lattice defects, which change the potential and hence charge carrier distribution near the surface. The sensitivity to gases, and the time dependence of response, is further modified in a porous body because this behaves as a complex network in which part of the conductivity, that modified by the surface interaction, is gas sensitive, whilst another part, that contributed by the 'bulk' sufficiently far from any surface, is not gas sensitive.[13] Such effects complicate the interpretation of data obtained on porous artifacts. Despite such complications, Williams and Moseley[14] showed that there was a general framework within which the behaviour of semiconducting oxides as reactive gas sensors could be understood. Oxygen species act as surface acceptors; if the bulk oxide is n-type then a decrease in the surface acceptor density increases the conductivity whereas if the bulk material is p-type then a decrease in the oxygen surface acceptor density decreases the conductivity. Behaviour which changed from apparently p-type to n-type with change of gas concentration or temperature could easily be rationalised using this model. The first report of CTO as a p-type sensor material for reactive gases was made by Moseley and Williams,[15] who claimed that it was selective to ammonia in air. Subsequently, the properties of CTO as a sensor material for H_2S in air were described by Dawson *et al.*[16] and by Henshaw *et al.*[5] A surface conditioning caused by sulfation and hydroxylation of surface sites was demonstrated, and a model for the sensor action based on reaction of surface oxygen species (O_{ads}^-) to form surface sulfate was developed. Sensors based on this material have been introduced commercially for detection of carbon monoxide in air, and for hydrocarbons and VOCs.[1] Williams and Pratt[17] described in outline the response of CTO to CO, acetone and toluene in air, and to ethanol, and assumed a response mechanism involving reaction of the target gas with doubly-occupied oxygen surface states (O^{2-}_{ads}), by analogy to the mechanisms proposed for the response of SnO_2. More information is available in the commercial literature.[1] Jayaraman *et al.*[6] reported responses to NH_3, H_2 and LPG, showing a response to ammonia increasing with increasing mole fraction of TiO_2 , to a maximum at approximately $Cr_{1.8}Ti_{0.2}O_3$.

Experimental

Materials preparation and measurement. Materials were prepared by solid-state reaction of Cr_2O_3 and TiO_2. Preliminary work showed that the degree of reaction was sensitively dependent on the particle size and mixing of the two powders, an effect which probably explains the discrepancies in the literature. With sufficiently small and well dispersed particles (for example by mixing colloidal dispersions of $Cr(OH)_3$ and TiO_2, drying and firing), complete reaction can be obtained in relatively short time at comparatively low temperature. A convenient procedure is the following: Cr_2O_3 in the form of a fine powder with typical particle size 50 nm was prepared by careful thermal decomposition in air of ammonium dichromate contained in a large flask fitted with air condenser and dust trap (*DANGER: EXPLOSION HAZARD. The temperature should be raised slowly to the ignition point, then the heating ceased. The amount of material decomposed at any one time should be limited*). The powder was dispersed in propan-2-ol and the required amount of titanium propan-2-oxide solution in propan-2-ol was added under ultrasonic agitation. After five minutes 5 cm^3 of water were added. After stirring under ultrasonic agitation for another 15 minutes the solvent was evaporated under reduced pressure in a rotary evaporator, with continuing ultrasonic agitation, and the powder was dried at 120 °C for two hours. Subsequently the powder was fired in recrystallised alumina crucibles for twelve hours at 1000 °C. The powder diffractometry and XPS methods were conventional; the method of measurement of gas-dependent conductivity (2-terminal measurements on pressed, porous pellets) has been described before.[5,18]

Computational methods. We recently carried out a study of antimony segregation on the (110) and (001) surfaces of SnO_2[19] and have used a similar strategy to address segregation in

Table 1 Potential parameters used for atomistic modelling

Chromium charge	+2.03	Shell charge	+0.97
		Spring constant/eV Å^{-2}	100.0
Titanium charge	+4.00	Shell charge	0
		Spring constant/eV Å^{-2}	0
Oxygen charge	+0.18	Shell charge	−2.18
		Spring constant/eV Å^{-2}	27.29

Table 2 Buckingham parameters used in atomistic modelling (potential energy of interaction, V_{ab}, of species a and b at distance r_{ab}: $V_{ab} = A\exp(-r_{ab}/B) - C/r_{ab}^6$

Interaction	A/eV	B/Å	C/eV Å^6
O^{-II}–Cr^{III}	1734.1	0.301	0.00
O^{-II}–Cr^{VI}	985.8	0.301	0.00
O^{-II}–O^{-II}	22764.3	0.149	27.88
O^{-II}–Ti^{IV}	2549.4	0.299	0.00

chromia. Having relaxed the cell using the shell-model with inter-ionic Buckingham potentials due to Lawrence[20] (Tables 1 and 2), we identified the most stable terminations for the (0001) and (10$\bar{1}$2) surfaces. The (10$\bar{1}$2) has been previously identified as the most stable surface (and therefore one would expect the least reactive), whilst the (0001) surface is less stable, but is well characterised experimentally since it is easily formed *via* epitaxial growth processing. We then relaxed each surface using a two-region approach, where the lower layer is fixed at the bulk geometry, whilst the upper layer is free to relax. The bulk geometry optimisation was carried out using the GULP software,[21b] whilst the surface relaxation was performed with the MARVIN code.[21a] The electrostatic summation for surfaces is more correctly described by a 2-D rather than a 3-D approach: hence the use of separate codes.

The aim of the simulation work was to explore the stability of charge neutral defect complexes at the two surfaces, of which two are considered here; Cr^{VI}–V_{Cr}''' and $(Ti^{\bullet}_{Cr})_3$–V'''_{Cr} The titanium potentials were from Grimes.[22] In carrying out segregation calculations, an important consideration is the periodicity of the surface repeat unit. For a low density of impurity, it is essential to choose surface repeat vectors that are sufficiently large to render periodic imaging effects negligible. Conversely, for a high density of impurity one may use a minimal surface repeat unit for the simulation. In the case of the (10$\bar{1}$2) face we used surface vectors of 4 × 1, whilst for the (0001) surface a 3 × 3 expansion was used, such that the shortest repeat vector was in excess of 15 Å. The simulation cell contained between approximately 2000 and 3000 ions.

Results

1. Phase characterisation

Powder diffractometry (Fig 1) of compositions having up to $x \approx 0.3$ showed a single phase material with lattice parameters very similar to Cr_2O_3, as reported by Jayaraman *et al.*[6] The lattice parameter variation shown by Oyama *et al.*[7] was not observed. A single diffraction line due to a second phase was just discernable at $x \approx 0.3$. This phase was clearly present at $x = 0.5$ and tentatively identified as $CrTiO_3$. XPS showed a strong Ti surface segregation (Fig 2), a characteristic splitting of the Cr2p$_{3/2}$ signal, (Fig 3a), a shoulder on the side of the Cr2p signals attributed to Cr^{VI}, Fig 3a, and the clear signature of the Cr3d states at the valence band edge (Fig 4). All of the signals were affected in a characteristic way by Ti substitution. The Cr states at the valence band edge diminished relatively in intensity. With a small Ti substitution, the valence band edge was moved by 0.3 eV referenced to the C1s peak at 285 eV. Further increasing titanium concentration moved the valence band up to 1.2 eV relative to the position for Cr_2O_3. The Cr^{VI}

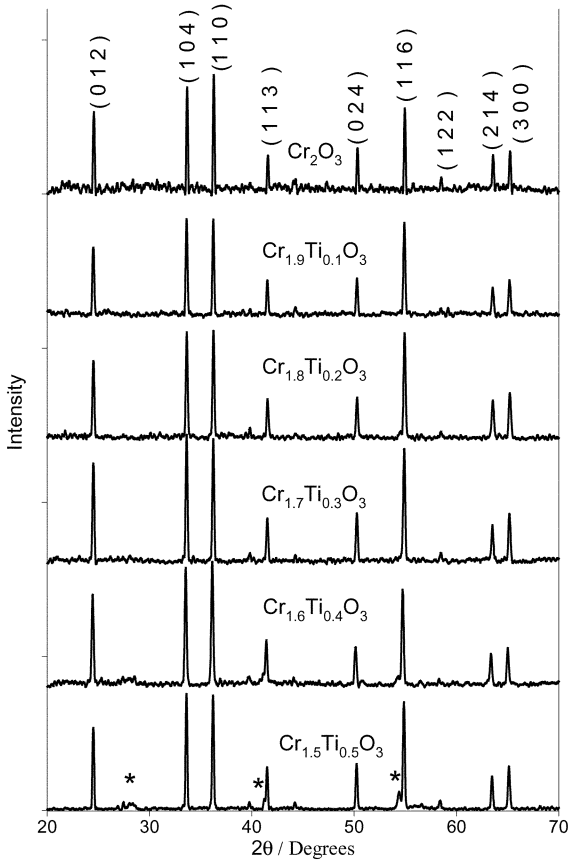

Fig. 1 X-Ray powder diffraction patterns of $Cr_{2-x}Ti_xO_3$, $0 < x < 0.5$. (* = second phase, identified as $CrTiO_3$ by the match of the observable diffraction peaks to JCPDS pattern 33–408).

signal was decreased relative to that of Cr^{III}: there was a strong effect of small Ti substitution, causing a decrease of the ratio $Cr^{VI}/(Cr + Ti)$ from 0.13 ± 0.02 for Cr_2O_3 to 0.08 ± 0.02 for $Cr_{1.99}Ti_{0.01}O_3$. This ratio remained constant with further increase of Ti substitution (Fig. 3b). The data for surface composition as a function of Ti substitution were fitted to the simple Langmuir–McLean model for segregation, which assumes constant Ti concentration equal to the bulk concentration up to the cation layer immediately below the surface and a coverage-independent Gibbs energy of segregation, and which gives a description of segregation to free surfaces of oxides which is not too inaccurate.[23] With this model, the

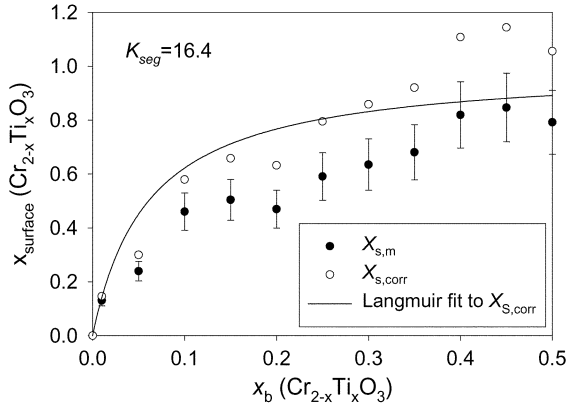

Fig. 2 Surface cation mole fraction of Ti, $x_{surface}$, against cation mole fraction of Ti in the preparation, x_b: the measured surface values are $x_{s,m}$ (error bars estimated from the counting and quantification uncertainties in XPS); values corrected assuming Ti composition uniform and equal to the bulk composition at all positions below the surface layer are $x_{s,corr}$.

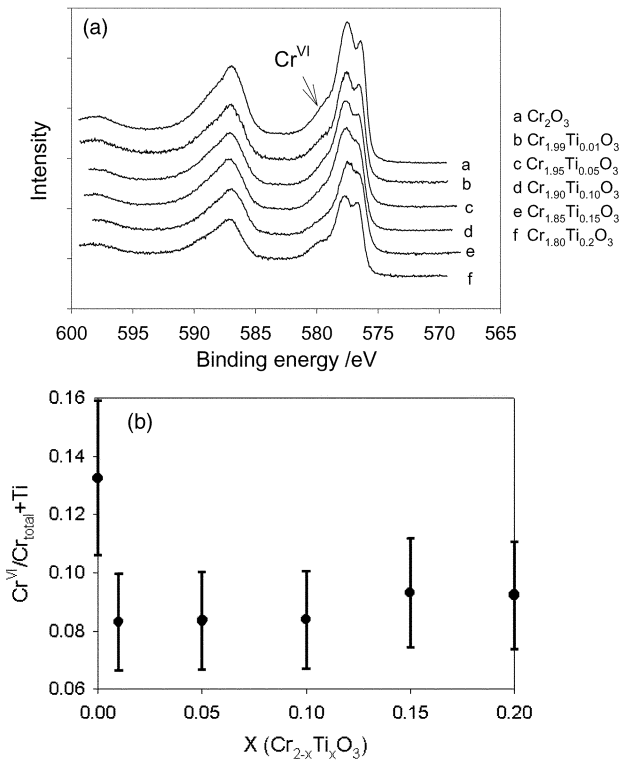

Fig. 3 (a) X-Ray photoelectron spectra of $Cr_{2-x}Ti_xO_3$ in the Cr 2p core region; (b) Surface cation fraction of Cr^{VI} as a function of the mole fraction of Ti in the preparation.

measured XPS signal was corrected for the signal due to sub-surface Ti taking the mean free path of Ti photoelectrons to be 1 nm and the thickness of the surface layer equal to the interlayer spacing in Cr_2O_3. The surface tends towards a composition having Cr/Ti = 1. The data (Fig. 2) gave an equilibrium constant for segregation, $K_{seg} \approx 16.4$, and hence the Gibbs energy of segregation, $\Delta_{seg}G \approx -RT_{calcine}\ln K_{seg} \approx -0.3$ eV. Here $T_{calcine}$ denotes the temperature of calcination of the powder during synthesis (1273 K).

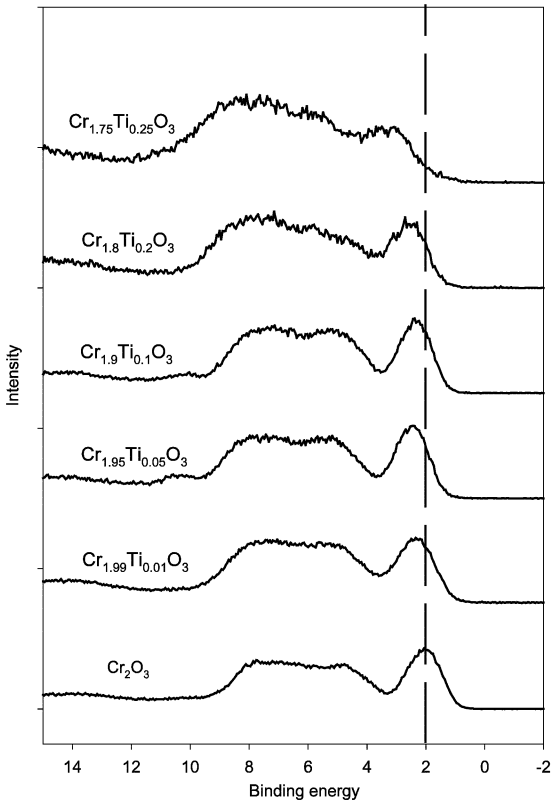

Fig. 4 X-Ray photoelectron spectra of $Cr_{2-x}Ti_xO_3$ in the valence band region.

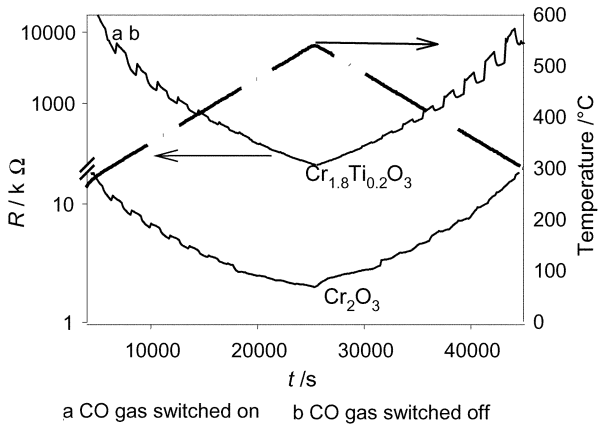

Fig. 5 Resistance, R, of porous pellets of Cr_2O_3 and $Cr_{1.8}Ti_{0.2}O_3$ as a function of time with change of temperature and gas atmosphere. The temperature changes linearly with time, from room temperature up to 550 °C and back down, and the gas is alternately switched between dry air and dry air containing 500 ppm of carbon monoxide. The resistance increases in the presence of CO in air. Pellet diameter 13 mm; pellet thickness approximately 2 mm. At the start of the experiment, the pellet is in equilibrium with room air, and dries in the stream of dry air as the temperature is increased.

2. Electrical behaviour and gas response

Important qualitative features of the behaviour as determined on porous pellets are shown in Fig. 5. This diagram illustrates that the substitution of a small amount of Ti into Cr_2O_3 caused a significant increase in resistivity and in activation energy of the resistivity, and the appearance of a significant gas response to carbon monoxide in air. Fig. 6 illustrates the variation of activation energy with Ti mole fraction and confirms the agreement of our work with the previous report.[5] Measurements at constant temperature showed that there was, in fact, a small response of resistivity of Cr_2O_3 to traces of CO in air but that this signal disappeared at temperature $\geqslant$ 300 °C. The effect of Ti substitution was to give a much larger gas response evident at higher temperature. The conductivity varied as $P_{O_2}^{1/4}$ and the gas response (ratio R/R_0 with R denoting the resistance in the presence of the target gas and R_0 that in the absence of target gas in air) varied approximately as the square root of the

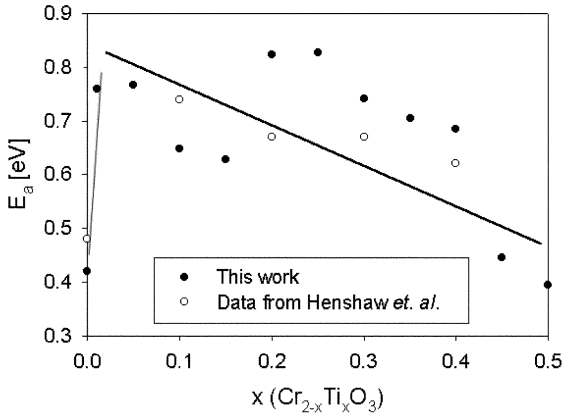

Fig. 6 Activation energy of conductivity compared with results reported in ref. 5.

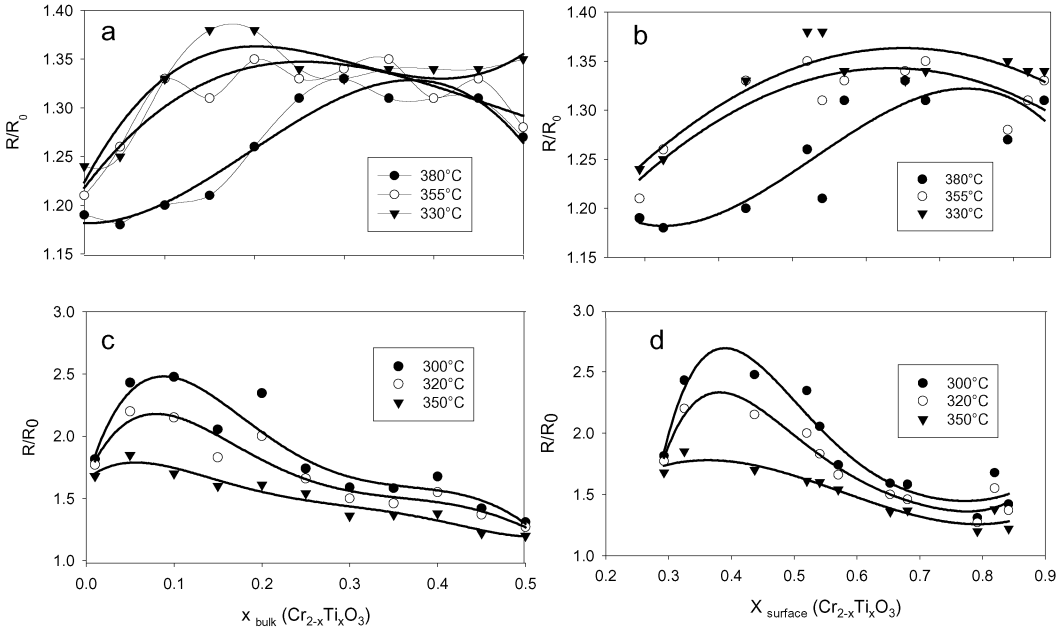

Fig. 7 Gas response expressed as R/R_0 , where R denotes the resistance in gas and R_0 that in clean dry air, (a, c): as a function of bulk composition (determined by energy dispersive X-ray analysis in the scanning electron microscope); (b, d) as a function of surface composition (determined by XPS). (a, b): gas is air saturated at room temperature with water vapour; (c, d): gas is 500 ppm CO in dry air.

gas concentration. This functional form is frequently found and attributed to involvement of O^{2-} states in the surface reaction, giving a variation of the charge carrier concentration at the interface with the square root of the gas concentration.[11,17] However, for resistance increasing response, the same functional form can arise simply because of the effect of the microstructure in modifying the observed response, when the charge carrier concentration at the interface varies linearly with the gas concentration:[13] hence no reliable conclusion concerning the stoichiometry of the surface reactions can be drawn. Fig. 7 shows the dependence of gas response on Ti substitution, again emphasising that only a very small substitution of Ti is necessary to achieve the gas response. Devices fabricated by screen printing show qualitatively similar behaviour to the pellets but with substantially larger and more rapid gas response because of their more open microstructure. What is practically significant about these devices is the rather small effect of variation in water vapour pressure upon the baseline and response, in comparison with the effects of gases such as CO. These effects are illustrated in Fig. 8. The variation of response to water vapour and to carbon monoxide with variation of titanium substitution was different. The response to carbon monoxide reached a maximum for $x \approx 0.05$ and then declined with further increase of Ti substitution, whereas the response to water vapour went through a broad maximum at $x \approx 0.2$, similar to the behaviour reported for response to NH_3 by Jayaraman *et al.*[6] The important fact relevant to the gas response is the strong surface segregation of Ti. The maximum in response to CO is at a surface cation concentration ratio $x_{surf} = [Ti]_{surf}/([Ti]_{surf} + [Cr]_{surf}) \approx 0.23$, and for water vapour it is at $x_{surf} \approx 0.5$

3. Computational studies

We carried out a systematic study of the stability of two charge neutral complexes (Cr^{VI}–V_{Cr}''' and $(Ti)_3$–V_{Cr}) in the bulk, $(10\bar{1}2)$ and (0001) surfaces using energy minimization techniques. To evaluate the stability of the defect complexes in the crystal bulk, we calculated the isolated defect energies using a Mott–Littleton strategy embodied in the GULP software. The defect energies relative to the perfect crystal are given in

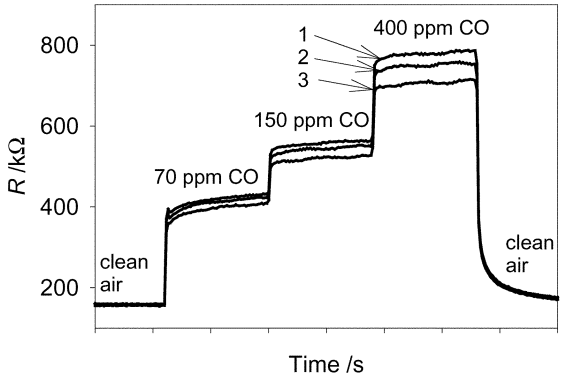

Fig. 8 Resistance, R, of a thick film sensor device operating at 400 °C in atmospheres of different relative humidity: 1, 50%; 2, 25%; 3, 10% RH at 20 °C

Table 3. The most stable charge neutral Ti^{IV}–V_{Cr} defect in bulk $Cr_{2-x}Ti_xO_3$ was a cluster of three Ti^{IV} in a trigonal arrangement surrounding a Cr vacancy; similar structures have been proposed by Grimes[22] for Ti doped alumina. Similarly, the most stable configuration of a Cr^{VI}–V_{Cr}''' complex was found to be an 'associated' state, where the vacancy and impurity are adjacent in the lattice.

The $(10\bar{1}2)$ and (0001) were fully relaxed and the significant interlayer relaxations shown by previous experimental[24] and *ab-initio* theoretical studies[25] of the perfect (0001) surface of Cr_2O_3 were reproduced in the present calculations. This result suggests that the driving force for the relaxation is electrostatic.

We firstly considered segregation in the $(10\bar{1}2)$ surface, which is known to be the most stable surface. Systematic exploration of the complex in various configurations within the lattice showed that segregation of the Cr^{VI}–V_{Cr}''' species was unfavourable, as shown in Table 3: that is, the complex would be expected to remain in bulk. Our calculations on the segregation of Ti are not definitive: the energy of the complex was found to decrease as it was moved from the bulk towards the surface, however with the potential model used here the calculations would not converge satisfactorily if the defect was placed on the

Table 3 Computed defect formation and segregation energies

Cluster	Bulk defect energy/eV	Segregation energy to (0001)/eV	Segregation energy to $(10\bar{1}2)$/eV
3 Ti^{IV}/V_{Cr}'''	−44.86	−3.76	−2.38[a]
Cr^{VI}/V_{Cr}'''	−178.88	−1.66	+2.28

[a]Segregation from bulk to position 0.4 nm below surface; calculation did not converge when the defect was placed closer to the surface.

surface‡. The interpretation that we place on these results is that both defect complexes are likely to be greatly stabilised by the exposure of the sample to oxygen. It has been noted by York *et al.*[26] that each surface cation strongly absorbs an oxygen monoatom, which completes the coordination sphere of the cation.

We then considered the same defect complexes at the (0001) surface. By comparing the total energies for the defect in the bulk-like region of the surface, with those of various geometric permutations at the surface, it was established that the most energetically favourable location of this cluster was near the surface. We found that it was more favourable to create a trigonal $(Ti)_3$–V_{Cr} complex in the sub-surface metal layer, rather than the terminal metal layer. This phenomenon is presumably attributable to the Ti^{IV} ion preferentially adopting a fully coordinated quasi-octahedral environment underneath the uppermost later of oxygen atoms, an effect which is displayed in Fig. 9. The defect formation energies relative to the perfect crystal are given in Table 3. In the surface-segregated defect cluster, oxygen anions surrounding the chromium vacancy relax away from the vacancy and move up slightly out of the surface. The computed defect segregation energies given in Table 3 are much larger than $\Delta_{seg}G$ deduced from the composition dependence of surface concentration.

The energetics and optimal geometry of the defect pair Cr^{VI}–V_{Cr}''' in pure Cr_2O_3 were also explored. Again, the most stable state was an associated pair segregated to the surface, as shown from the defect formation energies and segregation energies given in Table 3. There was significant distortion of the surface oxygen configuration: the oxygen ions clustered closely around the Cr^{VI} and relaxed away from the chromium vacancy. As in the case of Ti^{IV}, the Cr^{VI} was located below the surface. An optimum spacing of approximately 5 Å for the chromium vacancy and Cr^{VI} was found. At larger separations, the oxygen atoms closest to the Cr vacancy were screened from favourable overlap with the electropositive Cr^{VI} ion. The optimised surface configuration for this cluster is illustrated in Fig. 10.

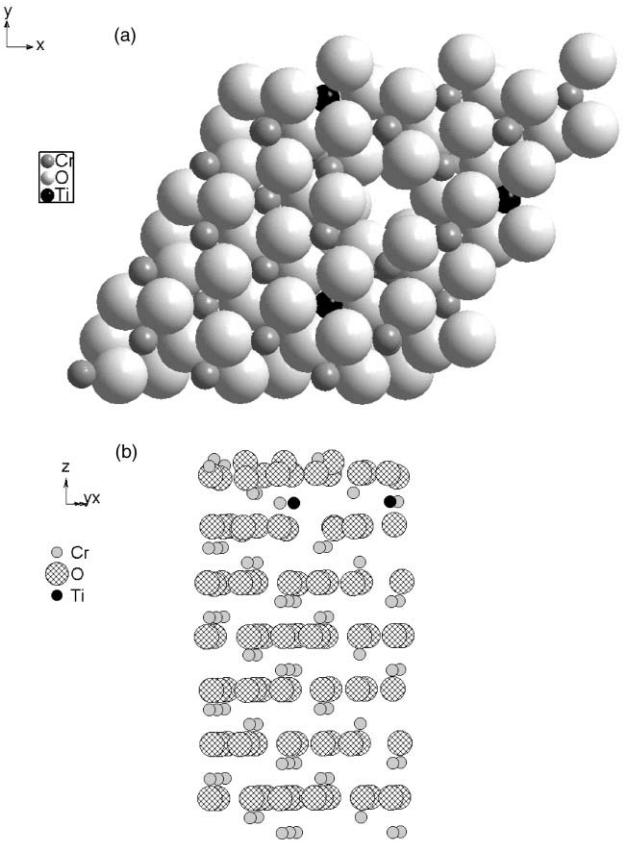

Fig. 9 (a) Computational model of (0001) face of CTO; three Ti^{IV} ions are charge balanced by a chromium vacancy; (b) View perpendicular to the (0001) face.

Discussion

1 Phase behaviour and surface composition

The existence of a solid solution of TiO_2 in Cr_2O_3 with a wide homogeneity range is confirmed. However, comparison with the high-temperature phase diagram[4] suggests that this phase has an upper stability temperature limit, which would be over 1000 °C (the preparation temperature used here) and below 1300 °C (the lowest temperature reported on the high temperature phase diagram). Oyama *et al.*[7] show much larger lattice parameter variations than we do. It is likely that their preparation has Ti uniformly distributed and is metastable because the powder was rapidly quenched from a high temperature whereas in ours the lattice strain caused by the defects is relieved by surface segregation. The computational results support this interpretation. They also reveal the strong stabilisation of the $(Ti)_3V_{Cr}$ complex, which can be interpreted that the material has a tendency to phase-separate, which would rationalise the difference between our results and the high-temperature phase diagram. It is notable that the surface composition tends towards a 1 : 1 mole ratio of Ti : Cr. The computed segregation energy is the enthalpy of segregation at 0 K and is significantly larger than the Gibbs energy of segregation deduced from the composition dependence of

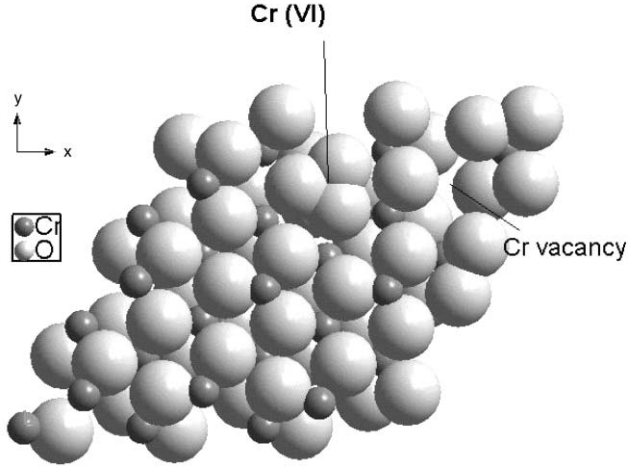

Fig. 10 Computational model of (0001) face of Cr_2O_3. A Cr^{VI} atom is charge balanced by a chromium vacancy.

‡The reason for lack of convergence is that formation of the complex on the surface is associated with considerable deviation from the ideal surface geometry of Cr_2O_3 . The rigid ion and shell model potentials used are fitted to reproduce perfect crystal structures but are transferable to environments which correspond reasonably closely in electronic and geometric state. The surface deformation and large electric fields at the surface induce polarization of such a magnitude that the linear response model of polarization, assumed by the shell model, is no longer valid.

surface composition (Fig. 2). The discrepancy between the segregation enthalpy calculated and that measured cannot be attributed to vibrational and configurational contributions to the segregation free energy, since these are generally fairly small.[23] Three factors may contribute: firstly, the simulation describes segregation at very low defect concentration whilst the experimental results refer to rather high defect concentration; secondly, the calculations refer to ideal surfaces and the experiment to the complex, polycrystalline, faceted interface characteristic of ceramic preparations; and thirdly, the inherent limitations of the interatomic potential models may lead to an overestimation of the segregation enthalpy. The experimental evidence that the measured mole fraction of Cr^{VI} decreased markedly with small Ti substitution but then remained constant we can interpret by proposing that Ti displaces Cr^{VI} from the top surface layer but that the Cr^{VI}–V_{Cr} defect remains segregated to the immediate sub-surface layers. A detailed description of the electrical behaviour would therefore have to take into account the contribution of these sub-surface acceptor states.

The Cr 2p splitting in XPS can possibly be interpreted as caused by a magnetic interaction with the unpaired spins localised in Cr 3d orbitals, induced by the deformation of the Cr environment at the surface and analogous to that found in Mn-based Heusler alloys[27] and in some ternary chromium sulfides and selenides.[28] The effect is not observable in the XPS of carefully prepared, single crystal $(10\bar{1}2)$ Cr_2O_3 surfaces, whilst it appears on (0001) surfaces (see below). The blurring of the lines caused by Ti substitution could then be explained by the deformation of the Cr environment near to the Ti, revealed by the computational modelling. The reappearance of the splitting at higher Ti concentration could then be attributed speculatively to ordering of the surface structure. However, this interpretation is not unambiguous since there is also a variation in the signal due to high-valent Cr which overlaps the Cr^{III} signals and causes an apparent broadening of the XP lines.

York *et al.*[26] have reported an experimental study of oxygen adsorption on the single crystal $(10\bar{1}2)$ surface of Cr_2O_3, which is Cr-terminated and the most stable crystal face. They reported that oxygen adsorbs dissociatively onto the surface, formally oxidising the surface Cr to Cr^{V}, completing the coordination shell of Cr and giving a completely oxygen-terminated surface. The dissociatively adsorbed oxygen was stable to over 1100 K. They identified this species with the chromyl species Cr=O which has been proposed to account for characteristic infrared absorption features of chromium oxide surfaces. Their results showed no splitting of the Cr $2p_{3/2}$ XPS signal and no indication of any change in the surface oxidation state of Cr through the appearance of any chemically-shifted emission line. On samples of chromia finely dispersed on alumina, on the other hand, where Cr might be found as isolated and oxidised atomic species,[29] signals attributable to Cr^{V} are readily distinguished.[30] Thus one concludes that states associated with Cr^{V} overlap the valence band of the bulk material so that the resultant holes are delocalised over the lattice, whilst there is a correlation energy which stabilises d^3 Cr^{III} and d^0 Cr^{VI} as localised, band gap states. A splitting[31] or broadening (at lower instrumental resolution)[32] of the Cr $2p_{3/2}$ signal from (0001) surfaces has been shown. The low binding energy peak is suppressed somewhat by oxygen adsorption and has been attributed[31] to Cr^{II} on patches of the surface which were Cr-terminated, or Cr^{II} in the immediate sub-surface, since these films were formed by oxidation of Cr under low pressures of oxygen in a vacuum system. EELS (electron energy loss spectroscopy) showed the Cr^{II} state completely removed by oxygen adsorption.[31] The XPS signal was still, however, evident in surfaces that had been dosed with Na, which forms surface Cr^{VI},[32] and is of course very clear on our samples, which have been formed by high-temperature sintering in air, a procedure which should have eliminated Cr^{II}. Thus the origin of the peak splitting for our samples remains somewhat uncertain.

2 Electrical behaviour

The relatively high conductivity of Cr_2O_3 can be attributed to the surface oxidation to Cr^{VI}. The computational results show that the Cr^{VI}–V_{Cr} defect pair is stable and strongly surface segregated. It would be further stabilised at the surface by interaction with adsorbed oxygen. These chromate or polychromate species have been observed by IR spectroscopy.[33–35] The empty Cr 3d states would act as electron acceptors, giving a p-type conductivity localised near the surface; the activation energy found for the pure porous Cr_2O_3, $\sim$0.4–0.5 eV, can be identified with the energy to excite a valence band electron into the empty Cr 3d states. The effect of Ti substitution, enhanced by its surface segregation, is to decrease the acceptor state density in the surface region and hence decrease markedly the conductivity. The activation energy found for specimens with small Ti substitution, $\sim$0.8 eV, is too small to correspond to band-gap excitation (3.3 eV, ref. 9). It could be attributed to the energy required to excite a valence band electron into a surface state associated with adsorbed oxygen, which decreases with increasing Ti substitution.

3 Gas response

The simplest phenomenological model is that the sensor material behaves as a parallel combination of a gas insensitive (the 'bulk') and a gas sensitive resistor (the surface) with some modification reflecting the influence of the microstructure.[13] Here, we interpret the conductive 'surface' element as due to both a surface layer of acceptor states associated with Cr^{VI} species and an accumulation layer of holes whose charge balances charge trapped in surface acceptor states. Oxygen adsorbed on the surface acts as the surface acceptor state: variation of the surface acceptor density as a consequence of reaction of surface oxygen with gas phase species is what confers gas sensitivity. If the acceptor concentration in the surface region is too large then variations of surface acceptor state density have little effect on the conductivity. The effect of Ti is then simply to diminish the concentration of surface-segregated acceptor states *i.e.* Cr^{VI}. Callister *et al.*[36] used the same interpretation to explain the effect of TiO_2 on the sintering rate of Cr_2O_3. The surface segregation of Ti is thus particularly important since it ensures that a small addition of Ti has a particularly marked effect. Ti present in the bulk, away from the surface would also have the effect of decreasing the bulk acceptor state density and hence of decreasing the conductivity of the gas insensitive 'bulk' element: since this shunts the gas sensitive 'surface' element, the effect would be to further enhance the gas sensitivity.

We have noted previously for a number of systems that the effects of water vapour are exerted on surface sites different from those involved in the gas response.[18,37,38] The same effect can be discerned in the present system: Fig. 7 shows the gas response and the response to water vapour plotted against the surface concentration of Ti. The gas response appears immediately there is sufficient Ti to neutralise the bulk acceptor states near the surface and then declines with further increase of the Ti content. The water vapour response on the other hand climbs to a maximum at $[Ti/(Ti + Cr)]_{surface} \sim 0.5$, corresponding to an overall composition of $Cr_{0.85}Ti_{0.15}O_3$. Since TiO_2 added in small amounts acts as a sintering aid for Cr_2O_3 and therefore results in a reduction in surface area (although the crystallite size indicated by X-ray diffraction line broadening is not increased), it is possible that the decline in signal with increasing Ti content is attributable to some degree to the effects of changing microstructure. However, differences in the behaviour of the CO and H_2O response to increase of Ti at low

Ti content implies a different interaction with the surface. One can speculate that H_2O is interacting predominantly *via* the Ti cations on the surface whereas the gas response appears predominantly as a result of an interaction involving both surface Cr and surface Ti. The decrease of surface Cr with increasing Ti therefore would cause a decrease in gas response, as observed.

4 Speculations concerning surface interactions mediating the gas response

We have previously noted that the surface sites which mediate gas response are different from those which mediate the major reaction paths for surface catalysed combustion.[38] This effect is particularly noticeable for the electrical response of CTO to carbon monoxide: on this material, in a flow-through packed bed reactor, there is no easily discernable catalysed combustion reaction of carbon monoxide at temperatures below 400 °C, in contrast to the behaviour of pure Cr_2O_3, which shows a strong catalysis of the reaction at temperatures below 200 °C.[29] However, the sensor signal on CTO is strong at the lower temperatures. Speculations on the active site for sensor response can be developed from other studies of the catalytic behaviour of chromium oxides and from our computational studies.

A generally accepted mechanism for redox catalysis on metal oxides, applicable to chromium oxide, is that of Mars and Van Krevelen[39] (M–vK)

$$M_{surf} + CO \rightarrow [M:CO]_{surf}$$

$$[M:CO]_{surf} + O_{latt,surf} \rightarrow M_{surf} + V_{O,surf} + CO_2$$

$$V_{O,surf} + \tfrac{1}{2}O_2 \rightarrow O_{latt,surf}$$

Burwell *et al.*[40] introduced the notion of the coordinatively unsaturated site, denoted above by M_{surf} to account for a gain in catalytic activity of Cr_2O_3 on heating. They proposed that these sites are exposed Cr^{III} surface atoms and that the activation of the catalyst is achieved by removal of water from those sites. Consequently adsorption of carbon monoxide and oxygen increases rapidly. For the case of CTO this effect leads to an increased gas response visible in Fig. 5 (right wing of the experiment). Cr_2O_3 shows the opposite behaviour, because the increased oxygen adsorption leads to increased formation of acceptor states, diminishing the gas response. Over *et al.*[41] provided an atomic-scale verification of the mechanism for CO oxidation on RuO_2. Vedrine *et al.*[42] pointed out that the M–vK mechanisms required sites having both redox and acid–base properties, particularly if hydrogen abstraction or oxygen insertion formed part of the reaction. They introduced the idea of a surface ensemble of ions constituting the active site, of particular structure: an inorganic molecular complex of a particular arrangement to promote a particular reaction. For oxidation catalysis on Cr_2O_3, the involvement of Cr^{III}–Cr^{VI} pair sites has been postulated, with adsorption onto Cr^{III} and electron transfer to adjacent Cr^{VI}.[43,29] We have recently considered the element of the reaction which involves the dissociation of molecular oxygen, showing that, in SnO_2, oxygen gas will dissociate at a bridging oxygen vacancy on the oxide surface, with one atom filling the vacancy and the other being adsorbed onto a coordinatively unsaturated (5-fold coordinated) surface Sn adjacent.[44]

Combination of these ideas with our computational studies of the chromium oxide surface suggests an interesting interpretation of the reactivity and gas sensor behaviour. These comments are necessarily qualified because we have limited our computational investigations to neutral defect complexes, as these can be relatively easily treated with atomistic techniques. First, we note that pre-adsorption of oxygen onto a clean, single crystal Cr_2O_3 (0001) surface has been shown to produce a surface which is rather inert to CO adsorption.[45] So, we propose that the chromium vacancy provides a site for carbon monoxide adsorption, promoted by the relaxation of the surface oxygen atoms away from the vacancy: the vacancy carries a net negative charge and CO is a dipole with oxygen positive, so it is plausible to suggest that CO adsorbs with oxygen down, in the pocket over the vacancy. Dissociation of the oxygen molecule is on Cr^{VI} or Ti^{IV}. The postulate is that oxygen is bound first as a peroxo species which then slowly dissociates: an analogous mechanism has recently been shown through computation to be feasible on Ti-substituted zeolites.[46] A complication for the application of this idea to the chromium oxide surfaces is that oxygen binds dissociatively and strongly to surface Cr cations,[26] and our modelling shows the Ti to be underneath the surface layer of oxygen. We can propose that the peroxo state derives from the low-coverage, weakly bound oxygen found on top of the surface layer[26] and that the dissociation involves a different and presently unspecified type of surface defect, where Cr^{III} and Ti^{IV} are exposed. The second adsorption site needed for an oxygen atom could be either adjacent Cr^{III} or the surface pocket formed over the Cr vacancy. The two surface oxygens would then constitute the surface electron trap states, one of which would be significantly more reactive than the other. Removal of these surface trap states is achieved by reaction with the carbon monoxide. (Scheme 1). Exposed Cr^{III} on the surface provides an extra adsorption side for carbon monoxide. Carbon dioxide is formed by reaction with oxygen, adsorbed on an adjacent Cr^{VI} or Ti^{IV} site. Reoxidation is now achieved by dissociation of an oxygen molecule between the Cr^{VI} or Ti^{IV} and an adjacent chromium vacancy. This is an M–vK mechanism in which the catalytic entity is a surface defect cluster. The difference in response for water vapour and for carbon monoxide is understandable if water is simply preferentially adsorbed onto the higher charge surface cations, rather than interacting with a pair of adjacent sites, one of which is associated with surface Cr and the other with surface Ti.

Conclusion

The gas sensing behaviour of $Cr_{2-x}Ti_xO_3$ is controlled by surface segregation of defect clusters. In the absence of Ti, one stable defect is a Cr^{VI}–V_{Cr}''' pair, which is surface segregated to (0001) and contributes to the relatively high conductivity shown by finely porous bodies of Cr_2O_3 at elevated temperature: the empty Cr 3d states act as electron acceptors, giving a p-type conductivity localised near the surface. The conductivity is dominated by the acceptor states associated with the high-valency Cr; any effect due to variation of the concentration of surface oxygen states, which is responsible for the gas sensing effect, is insignificant. With Ti addition, a stable defect, segregated to both (0001) and $(10\bar{1}2)$, is the complex $(Ti^{IV})_3V_{Cr}'''$. The effect of Ti substitution, enhanced by its surface segregation, is to decrease the surface concentration of the high-valency Cr species, that is to decrease the acceptor state density in the surface region. This is supported by the computational results which suggest that the surface segregation of the $(Ti^{IV})_3V_{Cr}'''$ complex is more thermodynamically favourable than segregation of the Cr^{VI}–V_{Cr}''' defect pair. The consequence is a significant decrease in electrical conductivity, which reveals the effects of variation in surface concentration of oxygen states and hence results in gas sensitive resistor behaviour. Distortion of the arrangement of surface oxygen above the Cr vacancy creates a potential binding site; the high-valency surface cation creates another. It is suggested that the two sites act in concert to promote the dissociation of oxygen and the surface reaction needed for gas sensing.

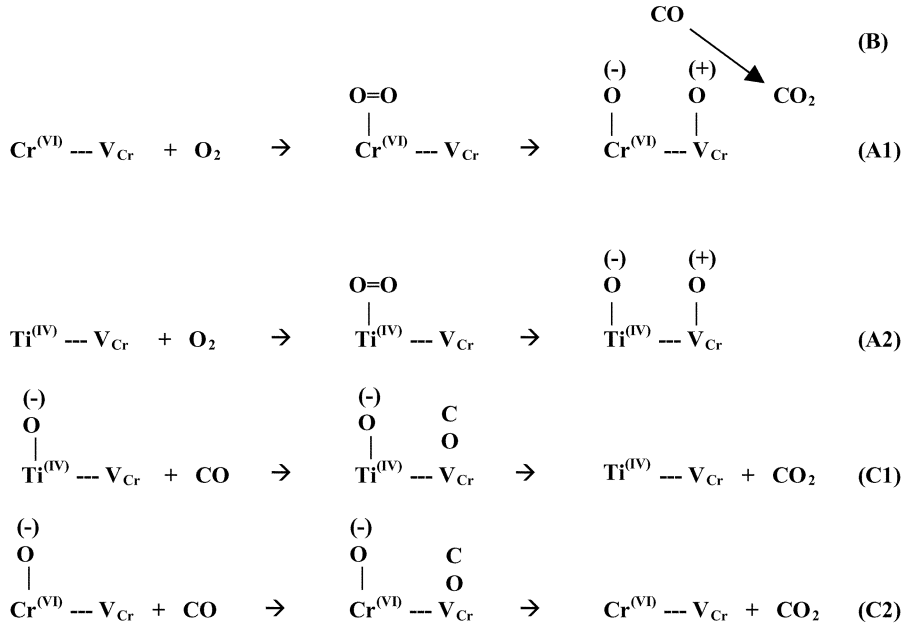

Scheme 1 Model for surface processes. Reactions A create reactive oxygen species which can also act as surface trap states for electrons. Reactions B remove the reactive surface oxygen species. Reactions C regenerate the initial surface state.

Acknowledgement

This work was supported by the Engineering and Physical Sciences Research Council, UK.

References

1 Capteur Sensors Ltd., Portsmouth, UK. http://www.capteur.co.uk/
2 S. Andersson, A. Sundholm and A. Magneli, *Acta Chem. Scand.*, 1959, **13**, 989.
3 S. Somiya, S. Hirano and A. Kamiya, *J Solid State Chem.*, 1978, **25**, 273.
4 *Phase Diagrams for Ceramists*, ed. A. E. McHale, Annual'91, National Institute for Standards and Technology, US Department of Commerce, Fig. 91-025; H. D. Werner, *Neues Jahrb. Mineral. Monatsh.*, 1974, 218.
5 G. S. Henshaw, D. H. Dawson and D. E. Williams, *J. Mater. Chem.*, 1995, **5**, 1791.
6 V. Jayaraman, K. I. Gnanasekar, E. Prabhu, T. Gnanasekaran and G. Periaswami, *Sens. Actuators, B*, 1999, **55**, 175.
7 T. Oyama, Y. Imura, T. Ishii and K. Takeuchi, *Nippon Kagaku Kaishi*, 1993, **7**, 825.
8 A. Holt and P. Kofstad, *Solid State Ionics*, 1999, **117**, 21.
9 A. Holt and P. Kofstad, *Solid State Ionics*, 1994, **69**, 127.
10 A. Holt and P. Kofstad, *Solid State Ionics*, 1994, **69**, 137.
11 D. E. Williams, in *Solid State Gas Sensors*, ed. P. T. Moseley and B. C. Tofield, Adam Hilger, Bristol, 1987.
12 A. Yamazoe and N. Miura, in *Chemical Sensor Technology*, ed. S. Yamauchi, Kodansha, Tokyo, 1992, vol. 4.
13 D. E. Williams and K. F. E. Pratt, *Sens. Actuators, B*, 2000, **70**, 214.
14 D. E. Williams and P. T. Moseley, *J. Mater. Chem.*, 1991, **1**, 809.
15 P. T. Moseley and D. E. Williams, *Sens. Actuators, B*, 1990, **1**, 113.
16 D. H. Dawson, G. S. Henshaw and D. E. Williams, *Sens. Actuators, B*, 1995, **26**, 76.
17 D. E. Williams and K. F. E. Pratt, *J. Chem. Soc., Faraday Trans.*, 1996, **92**, 4497.
18 V. Dusastre and D. E. Williams, *J. Mater. Chem.*, 1999, **9**, 965.
19 B. Slater, C. R. A. Catlow, D. H. Gay, D. E. Williams and V. Dusastre, *J. Phys. Chem. B*, 1999, **103**, 10644.
20 P. J. Lawrence, PhD Thesis, University of Bath 1988.
21 (*a*) D. H. Gay and A. L. Rohl, *J. Chem. Soc., Faraday Trans.*, 1995, **91**, 925; (*b*) J. D. Gale, GULP, version 1.3, Imperial College, 2001.
22 R. W. Grimes, *J. Am. Ceram. Soc.*, 1994, **77**, 378.
23 C. C. Battaile, R. Najafabadi and D. J. Srolovitz, *J. Am. Ceram. Soc.*, 1995, **78**, 3195.
24 F. Rohr, M. Baumer, H.-J. Freund, J. A. Mejias, V. Staemmler, S. Muller, L. Hammer and K. Heinz, *Surf. Sci.*, 1997, **372**, L291.
25 C. Rehbein, F. Michel, N. M. Harrison and A. Wander, *Surf. Rev. Lett.*, 1998, **5**, 337.
26 S. C. York, M. W. Abee and D. F. Cox, *Surf. Sci.*, 1999, **437**, 386.
27 S. Plogmann, T. Schlatholter, J. Braun, M. Neumann, Yu. M. Yarmoshenko, M. V. Yablonskikh, E. I. Shreder, E. Z. Kurmaev, A. Wrona and A. Slebarski, *Phys. Rev. B*, 1999, **60**, 6428.
28 V. Tsurkan, S. Plogmann, M. Demeter, D. Hartmann and M. Neumann, *Eur. Phys. J. B*, 2000, **15**, 401.
29 M. I. Zaki, M. A. Hasan and N. E. Fouad, *Appl. Catal., A*, 1998, **171**, 315.
30 K. Jagannathan, A. Srinivasan and C. N. R. Rao, *J. Catal.*, 1981, **69**, 418.
31 C. Xu, M. Hassel, H. Kuhlenbeck and H.-J. Freund, *Surf. Sci.*, 1991, **258**, 23.
32 J. S. Foord and R. M. Lambert, *Surf. Sci.*, 1986, **169**, 327.
33 I. R. Beattie and T. R Gilson, *J. Chem. Soc. A*, 1969, 2322.
34 J. A. Campbell, *Spectrochim. Acta*, 1965, **21**, 1333.
35 J. A. Campbell, *Spectrochim. Acta*, 1965, **21**, 851.
36 W. D. Callister, M. L. Johnson, I. B. Butlaer and R. W. Ure Jr., *J. Am. Ceram. Soc.*, 1979, **62**, 208.
37 V. Dusastre and D. E. Williams, *J. Mater. Chem.*, 1999, **9**, 445.
38 D. E. Williams and K. F. E. Pratt, *J. Chem. Soc., Faraday Trans.*, 1998, **94**, 3493.
39 P. Mars and D. W. van Krevelen, *Chem. Eng. Sci.*, 1954, **3**, 41.
40 R. L. Burwell, G. L. Haller, K. C. Taylor and J. F. Read, *Adv. Catal.*, 1969, **20**, 1.
41 H. Over, Y. D. Kim, A. P. Seitsonen, S. Wendt, E. Lundgren, M. Schmid, P. Varga, A. Morgante and G. Ertl, *Science*, 2000, **287**, 1474.
42 J. C. Vedrine, J. M. M. Millet and J.-C. Volta, *Catal. Today*, 1996, **32**, 115.
43 A. Ellison, J. O. V. Outbridge and K. S. W. Sing, *Trans. Faraday Soc.*, 1970, **66**, 1004.
44 B. Slater, C. R. A. Catlow, D. E. Williams and A. M. Stoneham, *Chem. Commun.*, 2000, 1235.
45 H. Kuhlenbeck, C. Xu, B. Dillman, M. Hassel, B. Adam, D. Ehrlich, S. Wohlrab, H.-J. Freund, U. A. Ditzinger, H. Neddermeyer, M. Neuber and M. Neumann, *Ber. Bunsen-Ges. Phys. Chem.*, 1992, **96**, 15.
46 G. Sankar, J. M. Thomas, C. R. A. Catlow, C. M. Barker, D. Gleeson and N. Kaltsoyannis, *J. Phys. Chem. B*, 2001, **105**, 9028.